Superficies y vacío
ISSN: 1665-3521
alex@fis.cinvestav.mx
Sociedad Mexicana de Ciencia y Tecnología de Superficies y Materiales A.C.
México

Luna-López, J. A.; Carrillo López, J.; Vivaldo-De la Cruz, I.; García Salgado, G.; Flores Gracia, F.; Aceves-Mijares, M.
Optical properties of solar cells with SiO2 and silicon rich oxide with silicon nanoparticles
Superficies y vacío, vol. 23, agosto, 2010, pp. 40-44
Sociedad Mexicana de Ciencia y Tecnología de Superficies y Materiales A.C.
Distrito Federal, México

Optical properties of solar cells with SiO_2 and silicon rich oxide with silicon nanoparticles

J. A. Luna-López, J. Carrillo López, I. Vivaldo-De la Cruz, G. García Salgado, F. Flores Gracia
CIDS-ICUAP, BUAP
Ed. 103, Col, San Manuel, Puebla, Pue., México 72570

M. Aceves-Mijares
Instituto Nacional de Astrofisica Optica y Electrónica
Apdo. 51 Puebla, Pue. 72000, México
(Recibido: 18 de febrero de 2010; Aceptado: 01 de julio de 2010)

A study of comparison of the optical characteristics of silicon solar cells with a layer of silicon oxide (SiO_2) deposited by SILOX, and silicon solar cells covered with a silicon rich oxide (SRO) film obtained by LPCVD containing silicon nanoparticles (Si-nps) was made. To increase the density of nanoparticles and thus improve the red photoluminescence and the photocurrent, the SRO films were annealed at 1100 °C. Photoluminescence spectra and atomic force microscopy measurements of the silicon rich oxide films are presented and discussed, as well as current-voltage curves and spectral response of the fabricated solar cells.

Keywords: Solar cell; Silicon rich oxide; Nanoparticles; Photoluminescence; Atomic force microscopy

1. Introduction

Currently, the photovoltaic (PV) energy is one of the most attractive options to electricity generation in form clean [1] and renewable. However, the PV energy is not yet economical in comparison with the energy obtained through the conventional sources. One of the main reasons of the high cost of the PV modules is the cost of the base material, which consists of very high purity silicon wafers used in the modern technology of solar cells (SC) fabrication [2-3].

Diverse technological alternatives, like thin film solar cells [2,4], have been developed to try of reducing the costs. Nevertheless, these technologies are little satisfactory with respect to the efficiency obtained in the conventional solar cells. An alternative solution to reduce costs would be to increase the energy conversion efficiency to values greater than those corresponding to the conventional SC. To get these results, it would be necessary to develop more advanced SC structures.

One of the aims of this work was to increase the energy conversion efficiency of silicon solar cells by means of silicon rich oxide (SRO) films deposited on the SC surface. These films have the optical property of absorption below ~300 nm radiation (UV), so that the absorbed energy by the SRO film is then reemitted as red light (PL). Silicon SC have a greater response [5] in the spectral range from 500 to 1000 nm, so that the redshift of the short wavelengths offers an increase in the energy conversion efficiency of the silicon SC with no significant increase in the cost of fabrication.

In this paper, the electrical and optical parameters of silicon SC with SRO are compared with those for conventional SiO_2-covered silicon solar cells. SRO films were deposited by LPCVD technique. These films were annealed at 1100° C for increasing the density of Si-nps and thus to increase the photoluminescence (PL) in the red wavelength range [6]. In previous papers [7-10] we have reported a study on SRO films regarding silicon excess and density as well as Si-nps size. It was possible to see silicon nanocrystals (Si-nc) in SRO_{10}, SRO_{20} and amorphous silicon nanoclusters of SRO_{30} films with diameters of approximately 5, 2.5 and 1 nm, respectively. In this work SRO_{30} films were used. PL spectra and atomic force microscopy (AFM) images corresponding to SRO films are presented and discussed, as well as current-voltage (I-V) curves and spectral response of the solar cells fabricated.

Table 1. Solar cells with diferent thermal treatment (TT) time and thickness of SRO and SiO_2.

		P1	P2	P3	P4	P5	P6
SRO (nm)	80	X	X				
	500			X	X		
Thermal treatment 1100° C (min)	90	X		X		X	
	180		X		X		X
SiO_2 (nm)	500					X	X

corresponding author: jalbluna@siu.buap.mx
israelvivac@yahoo.com.mx

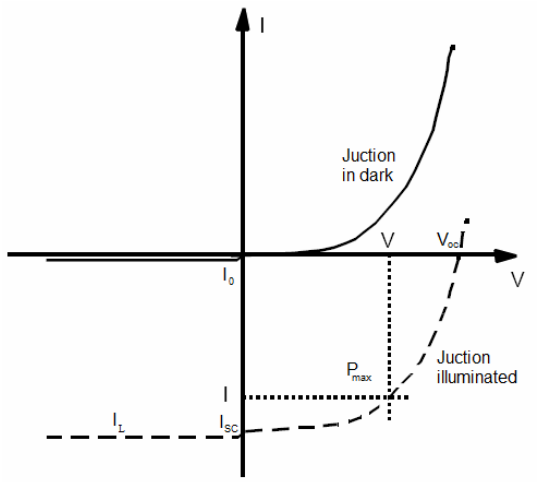

Figure 1. I-V curves for p-n junction in dark and illuminated operation modes.

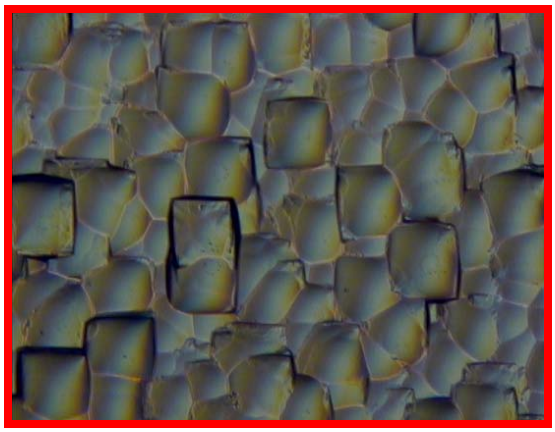

Figure 2. Photograph of the surface texture by anisotropic KOH attack.

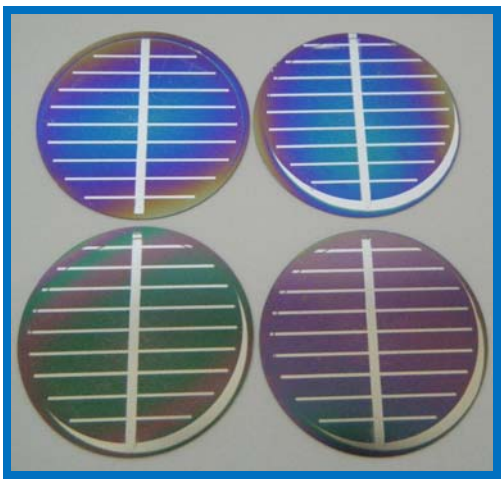

Figure 3. Photograph of the aluminum grids on the solar cell fabricated.

2. Theory

The measurement of current-voltage curve (I-V) provides the electrical characterization of a photovoltaic device. It is well known that the current through the solar cell under illumination is given by the equation $I = -I_L + I_o (e^{V/Vt} - 1)$ [11], where I_L is the current photogenerated by the effect of light and the second term is the junction current in darkness. When a solar cell is illuminated produces a region of operation where electrical power can be extracted from the device. In the condition of short circuit (V = 0), photogenerated current can be written in the form $I_{sc} = -I_L$, and open circuit voltage occurs when I = 0; in this case the equation is $V_{oc} = V_t \ln ((I_L/I_0) + 1)$, where V_t is the thermal voltage kT/q and I_0 is the saturation current for the junction.

The maximum theoretical power P_T, that can be obtained from a solar cell is given by the values of I_{sc} and V_{oc} ($P_T = V_{oc} * I_{sc}$), but the real power that a cell can provide to a load is given by the values of V and I, as shown in Figure 1, where $P_{max} = (V * I)$ max. The fill factor FF, represents a measure of usable power that can be obtained from a solar cell, and is defined as P_{max}/P_T.

The main characteristic of a solar cell is the energy conversion efficiency, which is an indication of the amount of solar power radiation that can be transformed to electricity. To obtain the energy conversion efficiency, it should be considered the voltage and current corresponding to the maximum power that the cell can provide to the load. The conversion efficiency of the solar cell is defined as the ratio of the maximum power generated by the cell to the power radiation, P_{in}, impinging on the solar cell surface, namely $(P_{max}/P_{in}) \times 100$ %.

The spectral response of a solar cell is defined as the output current in short circuit conditions per unit incident power of monochromatic light, as a function of the wavelength.

3. Experiment

SRO and SiO_2 were deposited on *p*-type silicon (100) substrates with resistivity of 9.5 Ω-cm, and 2 inches of diameter. SRO films were obtained in a horizontal LPCVD hot-wall reactor using SiH_4 (silane) and N_2O (nitrous oxide) as reactive gases at 715 °C. The gas flow ratio, Ro = $[N_2O]/[SiH_4]$, was used to control the amount of silicon excess in the SRO films. The structures of the solar cells designed are similar to the conventional cells with SiO_2; the only difference in this case is the SRO top layer instead of the SiO_2 layer. Before the SRO deposit, the surface of the silicon wafers was textured with potassium hydroxide (KOH) anisotropic attack for 21 minutes at 85 °C. Figure 2 shows the image of the textured surface; this is done in order to reduce the light reflection on the surface of the solar cell. Subsequently, the diffusion of phosphorus was realized at 875 °C for 30 minutes for the formation of the n region and thus obtaining the p-n junction. The surface of one group of solar cells (P1, P2, P3, P4) was passivated using SRO with two different thicknesses. Two other cells

(P5, P6) were covered with thermal SiO_2 deposited by SILOX; then, a thermal treatment at 1100° C for two times was given to all the samples, as indicated in Table 1.

Thermal treatments are performed with two purposes: one is the formation of silicon nanoparticles embedded in the oxide matrix of SRO, and the other is the phosphorus redistribution and thus to get the final junction depth in the solar cell. Finally, Aluminum grids were patterned on the SRO and SiO_2 surfaces by evaporation and standard photo-lithography as shown in Fig. 3. Aluminum grid electrodes on the surface have several fingers on all samples. It is important to remark that the zones between fingers are covered by the SRO films.

The surface morphology of SRO films was studied using a Nanosurf EasyScan atomic force microscopy (AFM) system version 2.3 operated in noncontact mode. A scanned area of 4 X 4 um^2 was used for each topographic image. Four different scans were done for each sample, showing good reproducibility. AFM images were analyzed using scanning image probe image processor (SPIP) software [12]. Room temperature PL of the SRO films was measured using a spectrofluorometer Horiba Jobin Yvon FluroMax 3 model with a xenon source of 150 W and a monochromator. The samples were excited using 290 nm radiation, and the emission signal was collected from 400 to 950 nm with a resolution of 0.3 nm.

Current-voltage (I-V) curves of the SC were obtained using a solar simulator and a curve tracer under AM1.5 conditions. Also, we obtained the current versus wavelengths (I-W) characteristic curves of the SC.

4. Results

Figure 4 shows the 3-D surface morphology of SRO films. The thermal treatment time strongly influences the size and density of grains so that a longer time of thermal treatment provoked more roughness and higher grains on the SRO surface.

Figure 5 shows results of the roughness analysis. It is clearly noted that with thermal treatment the roughness and diameter of the grains increases in both SRO and SiO_2 films. The results obtained by SPIP software with regard to grain diameter are listed in Table 2. The average roughness $<S_a>$ is defined in [12-13].

We used the red photoluminescence of the SRO films for increasing the number of photons reaching the active region of the SC. Figure 6 shows PL spectra of the SRO films. It is clearly noted that the samples with the shorter thermal treatment show a higher PL intensity. As mentioned above, this PL reemitted as red light by the SRO film will reach the active region of the p-n junction, thus increasing the solar cell photocurrent.

Figure 7 shows the spectral response in the visible and near infrared regions of the fabricated solar cells, where it is determined that the SC with SRO has a higher and better response than the cell with SiO_2. This fact confirms that the SRO is a material with good properties for applications in silicon solar cells technology.

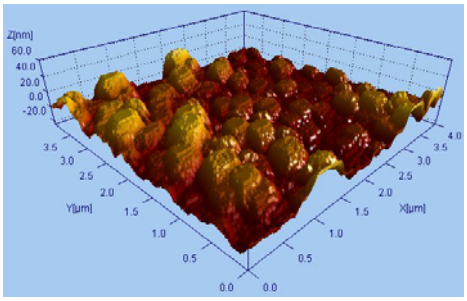

a) 90 minutes

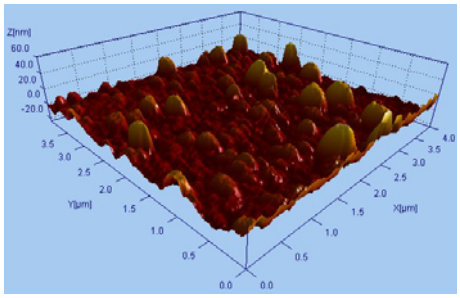

b) 180 minutes

Figure 4. 3-D image of SRO films with different annealing times at 1100° C. a) annealing time for 90 min, b) annealing time for 180 min.

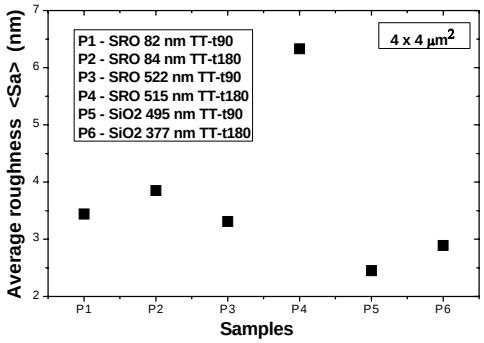

Figure 5. Average roughness of the SRO and SiO_2 films.

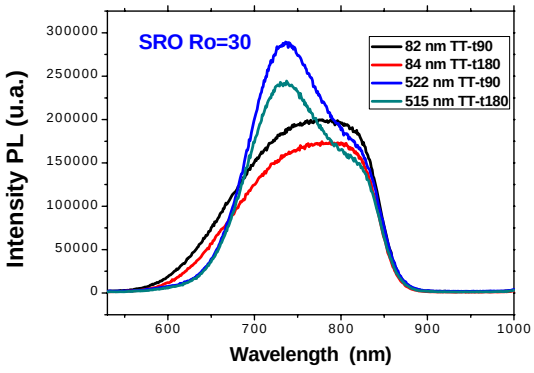

Figure 6. Photoluminescence Spectra of the SRO films deposited on the Solar Cell.

Figure 8 shows the I-V measurements from the silicon solar cells with SiO_2 and with SRO films. From these curves the open circuit voltage, short circuit current, fill factor and thus the maximum power can be obtained. These measurements were done using a solar simulator under AM1.5 conditions, and the I-V curves with the suitable hardware and software for the data processing.

5. Analysis and discussion

AFM measurements show that SRO films are more rugged than silicon oxide films. The surface roughness of SRO increases with the time of thermal treatment; this is because the silicon excess in the SRO film forms accumulations of silicon so that the thermal treatment at 1100° C favors the formation of grains at the surface, as shown in Figure 4. These results are consistent with those of other authors [13].

Photoluminescence of SRO films has been widely studied [6,14,15]. The two main mechanisms accepted for the generation of PL in the SRO, are the quantum confinement due to the nanocrystals, and defects present in the material. As shown above, SRO films show a high PL in the red.

One point of view in favor of SRO films is that they have a transmittance greater than 80% for wavelengths greater than 400 nm, so that the material does not absorb radiation with wavelengths from 500 to 1000 nm, and this radiation is absorbed by the silicon SC. Therefore, SRO films can be an excellent passivation material for SC, because they absorb short wavelength radiation (UV) and generate PL in the red region mainly, where the silicon SC has a higher spectral response. As shown in Figure 7, the solar cell covered with SRO (P2) has a better spectral response than the solar cell with SiO_2 (P5), in the visible and near-infrared regions.

From the characteristic I-V curves of the solar cells the following results were obtained: in the case of the cell passivated with SiO_2, it was found that I_{sc} = 9.26 mA/cm^2 and V_{oc} = 455 mV. From the cell covered with SRO the results were I_{sc} =22.2 mA/cm^2 and V_{oc} = 496 mV. Similar results as the last ones for I_{sc} and V_{oc} have been reported for silicon solar cells with quantum dots [16]. In this work, this is a first result and more research is necessary to get good parameters for the fabricated solar cells. However, this result in comparison with that of reference [16] is very good.

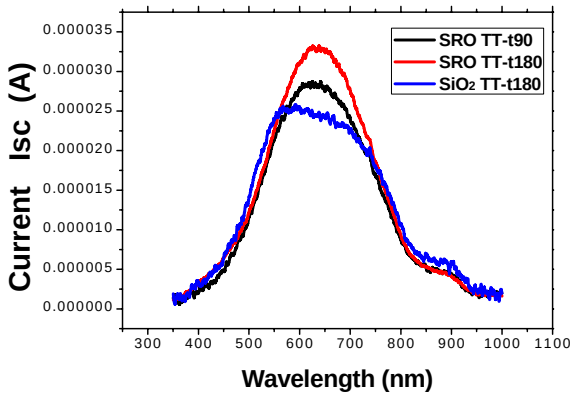

Figure 7. Spectral response of Solar Cells with SRO and SiO_2 films.

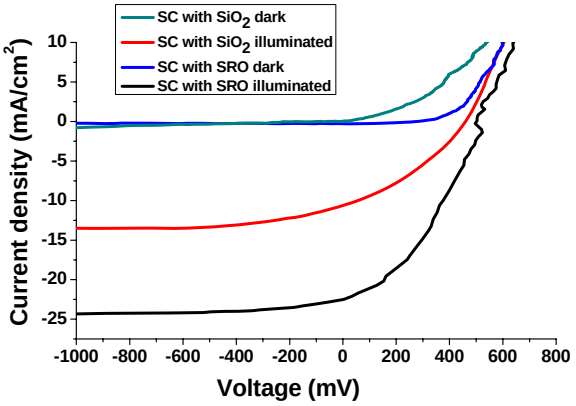

Figure 8. I-V curves of solar cells with SRO and with SiO_2 films.

According to the measurements of short circuit current and open circuit voltage, when the cells are illuminated under AM1.5 conditions, the SRO-passivated solar cells show a higher I_{sc} than the corresponding current for the cells with SiO_2.

Accordingly, the SRO is a better material than SiO_2 for this application on silicon solar cells; it is well known that the region between 500 and 900 nm is where the silicon solar cells have a better spectral response. With these results, it has been calculated an energy conversion efficiency for the SRO-passivated SC approximately three times higher than the corresponding efficiency for those with SiO_2.

Table 2. Characteristics of SRO films deposited on solar cells.

Sample	**Thickness** (nm)	**Time of TT at 1100° C** (min)	**Grain diameter** (nm)
P1	82	90	273
P2	84	180	250
P3	522	90	290
P4	515	180	443

6. Conclusions

From the analysis of AFM measurements we concluded that the better value for I_{sc} corresponds to the P2 SRO film with a surface roughness of 3.85 nm and grain diameter of 250 nm. The silicon solar cells passivated with SRO indeed showed better results than solar cell passivated with SiO_2 in the visible and near-infrared spectra. The increase in the efficiency is due to the absorption of high-energy photons (UV) within the SRO film and the subsequent reemission of red light to the body of the cell. The I-V characteristics for these cells showed very good results in open circuit voltage and short current values, so that their energy conversion efficiency was increased by ~ 200 % with respect to the SiO_2 – passivated conventional solar cell.

Acknowledgment

We would like to thank Consejo Nacional de Ciencia y Tecnología (CONACYT) and Vicerrectora de Investigación y Estudios de Posgrado **(**VIEP-BUAP) Project 2010 for providing support for this work. The authors also thank Pablo Alarcon, Manuel Escobar of the INAOE for helping in the samples preparation.

References

[1]. M.D. Archer, R. Hill (Eds.), Clean Electricity from Photovoltaics, Imperial College Press, London, 2001.
[2]. M.A. Green, Third Generation Photovoltaics: Ultra-High Efficiency at Low Cost, Springer-Verlag, 2003.
[3]. G. Conibeer, M. Green, R. Corkish, Y. Cho, E.-C. Cho, C.-W. Jiang, T. Fangsuwannarak, E. Pink, Y. Huang, T. Puzzer, T. Trupke, B. Richards, A. Shalav, K.-L. Lin, Thin Solid Films, **654,** 511–512 (2006).
[4]. J. De La Torre, G. Bremond, M. Lemiti, G. Gouillot, P. Mur, N. Buffet, Thin Solid Films **163,** 511 (2006).
[5]. A. L. Fahrenbruch, R. B. Bube, Fundamentals of Solar Cells, Photovoltaic Solar – Energy Convertion, Academic Press Inc, New York, 1983.
[6]. F. Iacona, G. Franzo, and C. Spinella, J. Appl. Phys. **87**, 1295 (2000).
[7]. J. A. Luna-López, M. Aceves-Mijares, O. Malik, Z. Yu, A. Morales, C. Dominguez and J. Rickards, Revista Mexicana de Física, **S 53 (**7), 293-298 (2007).
[8]. A. Morales-Sanchez, J. Barreto, C. Domínguez-Horna, M. Aceves-Mijares, J. A. Luna-López, Sensors & Actuators A, **142**, 12-18 (2008).
[9]. Ragnar Kiebach, José Alberto Luna-López, Guilherme Osvaldo Dias, Mariano Aceves-Mijares and Jacobus Willibrordus Swardt, J. Mex. Chem. Soc., **52**, 212-218 (2008).
[10]. Zhenrui Yu, M. Aceves-Mijares, A. Luna-López, Jinhui du and Dongcai Bian, Nanotechnololgy, **17**, 4962-4965 (2006).
[11]. M. A. Green, Solar Cells, Operating Principles, Technology, and System Applications. Prentice Hall, 1982.
[12]. J. F. Jogensen, SPIP, the scanning probe image processor, Denmark, 2002 (www.imagemet.com).
[13]. J. A. Luna- López, A. Morales-Sánchez, M. Aceves-Mijares, Z. Yu, C. Domínguez, J. Vac. Sci. Technol., A **27**, 57-62 (2009).
[14]. L. T. Canham, Appl. Phys. Lett. **57**, 1046 (1990).
[15]. H. Z. Song, X. M. Bao, N. S. Li, and J. Y. Zhang, J. Appl. Phys. **82**, 4028 (1997).
[16]. Eun-Chel Cho, Sangwook Park, Xiaojing Hao, Dengyuan Song, Gavin Conibeer, Sang-Cheol Park and Martin A Green, Nanotechnology, **19**, 245201 (2008).